Examination of the Dynamic Behaviour of the Composite Hollow Shafts Subject to Unbalance

Ala'a M. Al-Falahat
Department of Mechanical Engineering, Faculty of Engineering, Mutah University, Al-Karak, Jordan
Email: alaa.falahat@mutah.edu.jo

***Abstract*—The unbalance in rotating machines is one of the major sources of rotor damage. Therefore, providing information on the behaviours of the unbalance rotor shaft is necessary to avoid the early damage of the rotor shafts and improve the efficiency of the rotating machines. For this purpose, the dynamic behaviour of a rotating composite hollow shaft is investigated by analyzing the vibration of a homogenized finite element beam model contain a flexible composite hollow shaft and a solid disc through identifying the relationship between the rotor unbalance response with both magnitudes of the imbalance and the rotating speed of the rotor as a function of frequency response. The Campbell diagram and stability analysis of the composite shaft is investigated.**

***Index Terms*—rotating machine, unbalance rotor, composite hollow shaft, finite element**

I. Introduction

Rotating machinery is a significant subject that is widely used in many industrial and engineering fields such as, electrical motors and turbines or rotating shafts are some of the most commonly used ones in the aircraft gas turbine engine or the power generation [1-3]. In the modern-day industry, these machines are designed to operate at an increasingly excessive mechanical efficiency.

The composite materials have a valuable property compared with metals such as high strength to weight ratio and present higher associated damping that can induce a destabilizing effect [4, 5], which make them very attractive for rotation systems. Accordingly, the attempts are being made for replacing the metal shafts with composite ones in many applications such that cylindrical tube for automotive and driveshaft for helicopters, aerospace applications [6-8]

Rotor vibration is one main issue that limits these high-speed rotating machineries [9]. From one viewpoint, a higher rotation speed, the operating stress can increase significantly. On the other viewpoint, due to the manufacturing tolerances and different limitations, rotating machineries can't be perfectly balanced. Subsequently, as a combination of both issues, the vibration of the rotor can eventually cause a mechanical failure. The most common source that causes the system faults which is in general exist as a rotor unbalance, misalignment and cracks [10].

Rotor unbalance occurs in any rotating system when the axis of inertia does not coincide with a geometric axis (i.e., the system is "unbalanced") which produces a centrifugal force that operates at machine rotating frequency. This induces a deflection of the shaft and produces internal stress, influencing the working proficiency of the rotating system [2]. Vibration characteristics of unbalance response provide fundamental information for vibration control [11]. The response of the rotating system depends essentially on the mass distribution of the rotor, rotational speed, geometric proportion as well as on the dynamic stiffness of shaft, disks and bearings.

Accordingly, to avoid undesired vibration and enhanced reliability, understanding the dynamic behaviour of a rotor system subject to unbalance force is essential because the vibration caused by unbalancing might destroy the important parts of the machine such as bearings, gears and coupling. Therefore, an appropriate mathematical model of the system is performed to predict the natural frequencies, critical speed and system instability. Hence, early damage detection could be obtained.

Simulation and mathematical methods consider promising tool and adapted within numerous studies [12-20]. In this context, the present paper is applied to investigate the dynamic response of rotating the composite hollow shaft subjected to the various unbalance condition by developing a working mathematical model.

A. Basics of Rotor Dynamic

The understanding of the dynamic characteristic of rotating machines is crucial for both academic interest and industrial application. Before driving the equation of motions describing a rotor system, it is necessary to define the coordinate system. The coordinate systems and notations introduced would be used throughout this work as shown in Fig. 1.

Manuscript received December 27, 2020; revised March 21, 2021.

doi: 10.18178/ijmerr.10.10.572-576

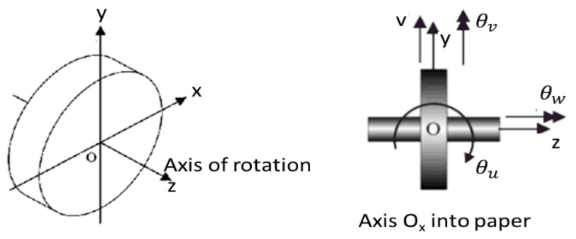

Figure 1. Coordinate system on a rotor.

The translation displacements along axis O_x, O_y, O_z that are described by u, v and w respectively, the clockwise rotation along O_x and O_y would be represented by positive θ_u and θ_v. Both of these two rotations were generally small compared to θ_w. Equation (1) gives the general form of the equation of motions for an n DOF system that represents the dynamic behaviour of a flexible rotor system.

$$[M]\{\ddot{q}\} + [C + \Omega C_g]\{\dot{q}\} + [K]\{q\} = \{F(t)\} \tag{1}$$

Where M is the mass matrix C is the damping matrix, C_g represents the gyroscopic effect and K is the elastic stiffness matrix, which was all $n \times n$ matrices and Ω was the rotational speed of the rotor. Displacements (u, v, θ_u, θ_v) in all DOFs were combined into a displacement vector (column vector) as [21] (i.e., the lateral vibration of the shaft). On the right-hand side was the unbalance force vector $F(t)$, in case of the free vibration $F(t)$ is equal zero.

In this work, the composite material is selected which gives two different matrices related with internal damping of the composite material as shown in Sino [21, 22], therefore the equation (1) is modified as:

$$[M]\{\ddot{q}\} + [C + \Omega C_g + C_i]\{\dot{q}\} + [K + \Omega K_i]\{q\} = \{F(t)\} \tag{2}$$

Where C_i and K_i internal damping matrix and stiffness matrix related to internal damping of the composite material. To enhance their dynamic behaviour, the anisotropic properties of composite materials can be used to develop composite hollow shafts.

The numerical model of the rotor system used in this work is extracted from Lagrange's equations and Rayleigh-Ritz method. The rotor is considered to by simply supported at both ends as shown in Fig. 2 by using bearing components as a simple support structure, also, the rotor mainly is formed of shaft and disk components.

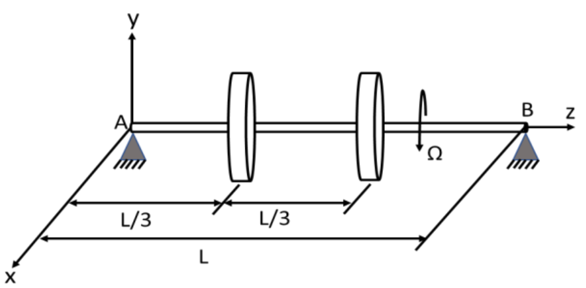

Figure 2. Schematic representation of the double-disk rotor.

Existing methods are considered the displacement along the x and y-direction (i.e., u and v, respectively), providing any z location along the shaft from 0 to L where L the length of the shaft as given in the following equation.

$$u(z,t) = \sum_{r=1}^{n} sin\frac{r\pi z}{L} q_{1r}(t) = sin\frac{\pi z}{L} q_{11}(t) + sin\frac{2\pi z}{L} q_{12}(t) + \cdots + sin\frac{n\pi z}{L} q_{1n}(t)$$

And;

$$v(z,t) = \sum_{r=1}^{n} sin\frac{r\pi z}{L} q_{2r}(t) = sin\frac{\pi z}{L} q_{21}(t) + sin\frac{2\pi z}{L} q_{22}(t) + \cdots + sin\frac{n\pi z}{L} q_{2n}(t) \tag{3}$$

Which $q_{1r}(t)$ and $q_{2r}(t)$ are the generalized independent coordinates and the function $\frac{\sin r\pi z}{L}$ are the displacement functions that represent the vibration modes related to each lateral direction of the selected rotor system [23, 24].

Fig. 1 shows also the angular rotations θ_u and θ_v around the directions x and y, respectively which can be estimated as follows:

$$\theta_u(z,t) = \sum_{r=1}^{n} \frac{d\left(\sin\frac{r\pi z}{L}\right)}{dz} q_{2r}(t)$$

And;

$$\theta_v(z,t) = -\sum_{r=1}^{n} \frac{d\left(\sin\frac{r\pi z}{L}\right)}{dz} q_{1r}(t) \tag{4}$$

The composite hollow shaft is considered a constant geometric property along its longitudinal z-axis. Therefore, the potential energy U_s of the shaft can be expressed by evaluation the integrals over the cross-section as given by Ref. [23]

$$U_s = \frac{1}{2}\int_0^L \left(EI_x \left(\frac{\partial \theta_u}{\partial z}\right)^2 + EI_z \left(\frac{\partial \theta_v}{\partial z}\right)^2 \right) dz \tag{5}$$

Which the homogenized flexural inertias are $EI = EI_x = EI_y$ for a circular section which is obtained based on the simplified homogenized beam theory (SHBT).

The total kinetic energy T_t of the composite shaft is the summing up of the kinetic energy of the shaft T_s, the disc T_D and the unbalance mass T_u included the translatory, rotary inertia and gyroscopic effect are given:

$$T_s = \frac{1}{2}\rho S \int_0^L (\dot{u}^2 + \dot{v}^2) dz + \frac{1}{2}\rho I \int_0^L (\dot{\theta}^2{}_v + \dot{\theta}^2{}_u) dz + \rho I L \Omega^2 + 2\rho I \int_0^L \dot{\theta}_v \theta_u dz \tag{6}$$

$$T_D = \frac{1}{2} M_D (\dot{u}^2 + \dot{v}^2) + \frac{1}{2} I_{Dy} (\dot{\theta}^2{}_v + \dot{\theta}^2{}_u) + \frac{1}{2} I_{Dz} (\Omega^2 + 2\Omega \dot{\theta}_v \theta_u) \tag{7}$$

$$T_u = m_u \Omega e (\dot{u}\, cos\Omega t - \dot{v}\, sin\Omega t) \tag{8}$$

Which ρ, S and I are the volumetric density, cross-section of the shaft and area moment of inertia of the shaft respectively. Besides, M_D, I_{Dx} and I_{Dz} are the mass of the disc, mass moments of inertia of the disc around the directions x and z. Also, as shown in Fig. 3, m_u is the unbalanced mass, and e is the eccentricity of the unbalance mass.

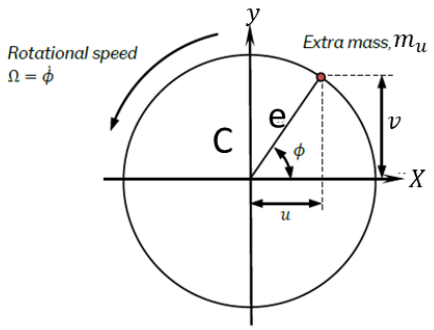

Figure 3. Instantaneous position of unbalance mass

Finally, by applying Lagrange's equation, the differential equations that represent the dynamic behaviour of the rotor system as follows.

$$\frac{d}{dt}\left[\frac{\partial(T_t)}{\partial \dot{q}_{ir}}\right] - \frac{\partial(T_t)}{\partial \dot{q}_{ir}} + \frac{\partial U}{\partial q_{ir}} \quad (9)$$

II. Simulation Modelling

A. Mathmatical Model

This project investigates how the unbalance force effect on the hollow shaft rotor response via simulation model. MATLAB code is used to develop a functioning of the mathematical modelling of the rotating system. The finite element model of an imbalanced rotor system is assembled. As shown in Fig. 4, the model is proposed by selecting 7 nodes on the rotor shaft that cause increased the number of Degree of freedom (DOF) and then more accuracy of the simulation results.

The whole shaft is segmented to 6 equalled elements with the length of $l_e = 0.15\ m$. The first and the seventh components are chosen to be the bearing at node 1 and 7 respectively which are represented to be a red trigonal around the shaft, the anisotropic spherical roller bearing type is used (8-ball bearing in this study) and the ratio of horizontal to vertical stiffness is 0.46.

The identical two disks are selected to be rigid steel ($\rho = 7800 \frac{kg}{m^3}$) and symmetric with 150 mm diameter and 20 mm thickness and the corresponding node of the disks are located at node 3 and 5. The inside diameter d_i of the disk is assumed to be the outside diameter of the shaft.

Using the equations presented previously, the key parameters for the system was calculated. The calculation process was fairly straightforward with geometrical dimensions and formulas provided, which would thus not be demonstrated here.

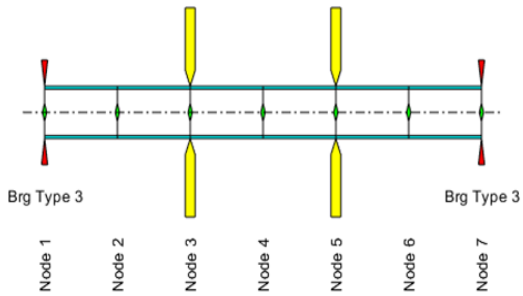

Figure 4. Simulation model layout

B. Composite Hollow Shaft

The composite hollow circular cross-section shaft was chosen in this work which is made by HM Carbon/Epoxy composite hollow shafts as shown in Fig. 5. This type of circular shaft is used where high strength and rigidity are required [25]. As a comparison, the hollow circular shafts are stronger in per kg weight than solid circular, also, the solid shaft has zero stress distribution at the and maximum at the outer surface while in hollow shaft stress variation is smaller [26].

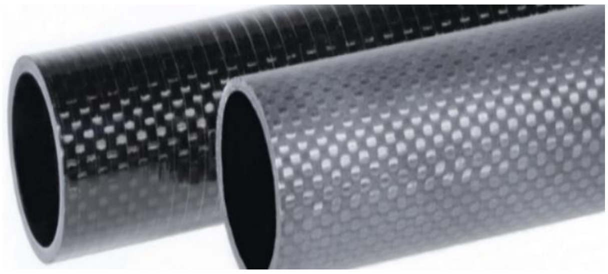

Figure 5. Composite hollow shaft provided by rock west composites [27].

Table I shows the mechanical and geometric properties of the analysed composite hollow shaft material.

TABLE I. Mechanical and Geometric Properties of the Composite Hollow Shaft

Property	Symbol	Value	Units
Young'smodulus of elasticity	E	90	GPa
Poisson's ratio	Y	0.14	-
Shear modulus	G	4.6	GPa
Density	P	1600	Kg/m^3
Outer diameter	d_o	25	mm
inner diameter	d_{in}	22.2	mm
Wall thickness	T	1.4	mm

The composite hollow shaft is designed by considering the number of layers as 3 and the stacking sequence 0/45/45 is selected as this stacking sequence more shear load could be applied on the shaft.

In this paper, a simplified homogenized beam theory (SHBT) is used to represent the dynamic behaviour of the hollow shaft [28]. The parameters given in table I are used to calculate the stiffness EI of the hollow shaft by using a demonstrated equation from Ref. [29].

III. Results

The simulation result of the constructed model is achieved by calculating their eigenvalue and eigenvector as shown in Fig. 6, the first four natural frequencies ω_i and corresponding mode shape is demonstrated, the calculated natural frequencies set of two, one of which was forward (left) whirl and the other being backward (right).

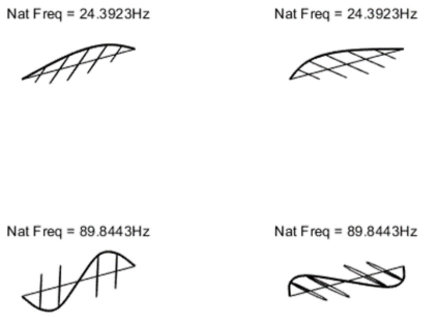

Figure 6. First four mode of the vibration mode.

Fig. 7 represents the Campbell diagram of the selected rotor system; the blue dot line demonstrates where is the spin speed intersected with the evaluated first four natural frequency range from the model. This point denotes critical speeds where is the maximum vibration response was expected to occur.

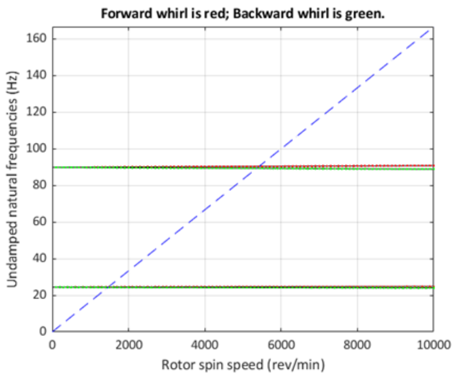

Figure 7. The Campbell diagram of the considered model

In this simulation, the selected rotating forces applied to the system by specifying the two identical unbalance masses were added onto each disk which was attached at a radius of 0.0625 mm from the rotating axis. There are three possible ways to change the magnitude of the centrifugal force that is expressed as $me\Omega^2$ by varying the rotation speed or the unbalance mass or change the eccentricity of the unbalance mass.

Using the numerical calculations, the results measuring at a bearing (node 1) were achieved as shown in Fig. 8.

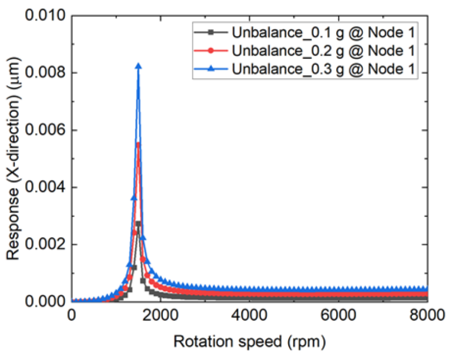

Figure 8. Output response spectra of a various unbalance mass at node 1 (lift bearing)

From the response spectrum shown above, the effect of increasing the magnitude of the unbalance mass at both rotors is noticed. It can be observed that with an increase in the imbalance mass, the magnitude of vibration characteristics increases, the reason for which can be attributed to an increase in centrifugal force produced during operation. Thus, it can be concluded that the magnitude of applied unbalance mass was proportional to which of the frequency response.

On the other hand, the effect of mass unbalance does not influence the magnitude of the natural frequencies of the system. The reason might be that although the unbalance would affect the mass matrix of the system, its magnitude used in this simulation was still insignificant comparing to the whole system.

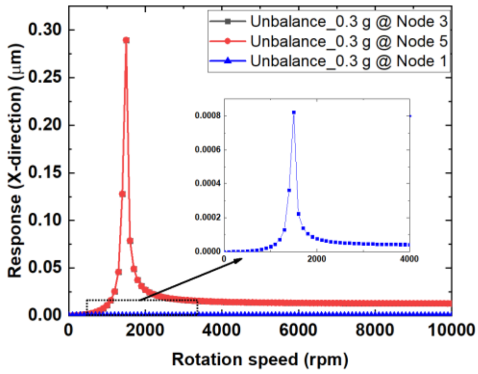

Figure 9. The output response of the considered model at the bearing, first disk and the second disk locations.

Fig. 9 shows the comparison between the response at the same unbalance mass, but at a different position along the shaft here, i.e. bearing, first disk and second disk are selected. It is seen that the maximum influence of the response is observed at both identical disks about 0.3 µm.

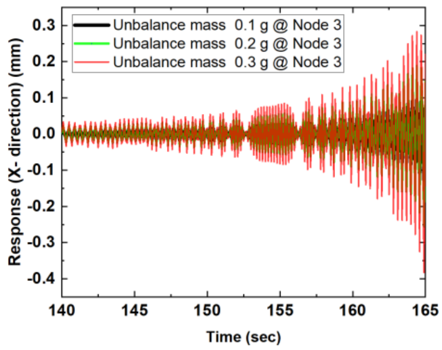

Figure 10. Vibration response of the considered model operation at 2000 rpm.

Fig. 10 shows the vibration response of the hollow shaft operation at 2000 rpm, as clearly seen the unstable condition is observed at node 9 (which is the x-axis of the first disk) by demonstrated the response of the three unbalance mass conditions through operation the rotor shaft at 2000 rpm. The simulation results were obtained from 0 to 165 sec in the step of 1 sec.

IV. Conclusion

The simulation of the dynamic rotor model was constructed based on the Lagrange's equations and the

Rayleigh-Ritz method, to investigate the dynamic behaviour of the rotating composite hollow shaft, also, the system response to the various magnitude to the imbalance force was investigated. In this context, the first four nature frequencies were obtained and the mode shape corresponding to the natural frequencies was found, the proposed analysis was implemented both in the time and frequency domains by represented the Campbell diagram, unbalance response and the instability threshold at a different rotor speed of the rotating composite shaft.

CONFLICT OF INTEREST

The auther declare no conflict of interest.

REFERENCES

[1] J. S. Rao, *History of Rotating Machinery Dynamics*, [Dordrecht]: Springer, 2014, pp. 45-47.

[2] M. David, L. Xiaochuan, B. Ian, and D. Fang, "Multidimensional prognostics for rotating machinery: A review," *Advances in Mechanical Engineering,* vol. 9, no. 2, 2017.

[3] T. K. Ibrahim *et al.*, "Study of the performance of the gas turbine power plants from the simple to complex cycle: A technical review," *J. Advance Res. Fluid Mechanics Therm. Sciences Journal of Advanced Research in Fluid Mechanics and Thermal Sciences,* vol. 57, no. 2, pp. 228-250, 2019.

[4] R. Sino, T. N. Baranger, E. Chatelet, and G. Jacquet, "Dynamic analysis of a rotating composite shaft," *Composites Science and Technology,* vol. 68, no. 2, pp. 337-345, 2008.

[5] S. Mayer, J. M. F. d. Paiva, and M. C. Rezende, "Comparison of tensile strength of different carbon fabric reinforced epoxy composites," *mr Materials Research,* vol. 9, no. 1, pp. 83-90, 2006.

[6] K. Gupta, "Composite shaft rotor dynamics: An overview," *Vibration Engineering and Technology of Machinery* Springer International Publishing, 2015.

[7] M. S. Darlow and J. Creonte, "Optimal design of composite helicopter power transmission shafts with axially varying fiber layup," *Journal of the American Helicopter Society,* vol. 40, no. 2, pp. 50-56, 1995.

[8] A. M. Falahat, M. A. Hamdan, and J. A. Yamin, "Engine performance powered by a mixture of hydrogen and oxygen fuel obtained from water electrolysis," *Int.J Automot. Technol. International Journal of Automotive Technology,* vol. 15, no. 1, pp. 97-101, 2014.

[9] R. King, *Flow Induced Vibrations*. [Place of publication not identified]: Springer, 1987.

[10] W. Ryan, P. Sureshkumar, and K. J. Ian, "Rotordynamic Faults: Recent Advances in Diagnosis and Prognosis," *International Journal of Rotating Machinery,* vol. 2013, 2013.

[11] J. X. Didier, J. J. Sinou, and B. X. Faverjon, "Study of the non-linear dynamic response of a rotor system with faults and uncertainties," *Journal of Sound and Vibration,* vol. 331, no. 3, pp. 671-703, 2012.

[12] S. S. Alrwashdeh, "Modelling of operating conditions of conduction heat transfer mode using energy 2D simulation," *International Journal of Online Engineering,* Article vol. 14, no. 9, pp. 200-207, 2018.

[13] S. S. Alrwashdeh, "Assessment of photovoltaic energy production at different locations in Jordan," *International Journal of Renewable Energy Research,* Article vol. 8, no. 2, pp. 797-804, 2018.

[14] S. S. Alrwashdeh, "Investigation of the energy output from PV racks based on using different tracking systems in Amman-Jordan," *International Journal of Mechanical Engineering and Technology,* Article vol. 9, no. 10, pp. 687-694, 2018.

[15] S. S. Alrwashdeh *et al.*, "In-situ investigation of water distribution in polymer electrolyte membrane fuel cells using high-resolution neutron tomography with 6.5 µm pixel size," *AIMS Energy,* Article vol. 6, no. 4, pp. 607-614, 2018.

[16] S. S. Alrwashdeh *et al.*, "Improved performance of polymer electrolyte membrane fuel cells with modified microporous layer structures," *Energy Technology,* Article vol. 5, no. 9, pp. 1612-1618, 2017.

[17] S. S. Alrwashdeh *et al.*, "Neutron radiographic in operando investigation of water transport in polymer electrolyte membrane fuel cells with channel barriers," *Energy Conversion and Management,* Article vol. 148, pp. 604-610, 2017.

[18] S. S. Alrwashdeh, H. Markötter, J. Haußmann, J. Scholta, A. Hilger, and I. Manke, "X-ray tomographic investigation of water distribution in polymer electrolyte membrane fuel cells with different gas diffusion media," in *ECS Transactions*, 2016, vol. 72, pp. 99-106.

[19] A. M. Al-Falahat *et al.*, "Energy-selective neutron imaging by exploiting wavelength gradients of double crystal monochromatorsSimulations and experiments," (in English), *Nuclear Instruments and Methods in Physics Research Section A: Accelerators, Spectrometers, Detectors and Associated Equipment Nuclear Instruments and Methods in Physics Research Section A: Accelerators, Spectrometers, Detectors and Associated Equipment,* vol. 943, p. 162477, 2019.

[20] A. M. Al-Falahat *et al.*, "Correction approach of detector backlighting in radiography," *The Review of scientific instruments,* vol. 90, no. 12, 2019.

[21] R. Sino, E. Chatelet, T. N. Baranger, and J. R. G., "Stability analysis of internally damped rotating composite shafts considering transversal shear," in *Proc. ISROMAC,* vol. 11, no. Honolulu, Hawaii USA 2006.

[22] J. K. Dutt and B. C. Nakra, "Stability of rotor systems with viscoelastic supports," *Journal of Sound and Vibration Journal of Sound and Vibration,* vol. 153, no. 1, pp. 89-96, 1992.

[23] M. Lalanne and G. Ferraris, *Rotordynamics Prediction in Engineering*, 2nd edition ed. Chichester Wiley 2001, 2001.

[24] R. R. Craig and A. J. Kurdila, *Fundamentals of Structural Dynamics*. Hoboken, NJ: John Wiley, 2006.

[25] M. B. P. M, "Design and analysis of composite drive shaft," *IJRASET International Journal for Research in Applied Science and Engineering Technology,* vol. 6, no. 5, pp. 1570-1576, 2018.

[26] I. V. S. Yeswanth and A. A. E. Andrews, "Parametric optimization of composite drive shaft using ansys workbench 14.0," *Int. J. Mech. Eng. Technol. International Journal of Mechanical Engineering and Technology,* vol. 8, no. 5, pp. 10-23, 2017.

[27] Rockwestcomposites. (2020, 04/10). *A global leader for all things composites*. [Online]. Available: https://www.rockwestcomposites.com/blog/carbon-fiber-grades-its-all-about-tensile-modulus/

[28] G. J. Kennedy and J. R. R. A. Martins, "A homogenization-based theory for anisotropic beams with accurate through-section stress and strain prediction," *International Journal of Solids and Structures,* vol. 49, no. 1, pp. 54-72, 2012/01/01/ 2012.

[29] R. Sino, T. N. Baranger, E. Chatelet, and G. Jacquet, "Dynamic analysis of a rotating composite shaft," *Composites Science and Technology,* vol. 68, no. 2, pp. 337-345, 2008.

Ala'a M. Al-Falahat received the B.E.,degree in 2007 and M.E. in 2012 both in mechanical engineering from Mutah University and Jordan university , Jordan, respectively. In 2015, he joined the Helmholtz zentrum berlin, Germany, and got the Ph.D from Technische Universität Berlin in 2019, he has been with the Department of mechanical engineering, where he is currently a Asisstant Professor. His resreach interest include rotordynamics, automatic control and mechanical vibration